Structural Signal of a Dynamic Glass Transition

Sudeshna Chattopadhyay,[1] Ahmet Uysal,[1] Benjamin Stripe,[1] Guennadi Evmenenko,[1] Steven Ehrlich,[2] Evguenia A. Karapetrova,[3] and Pulak Dutta[1]

[1]*Department of Physics and Astronomy, Northwestern University, Evanston, Illinois 60208, USA*
[2]*National Synchrotron Light Source, Brookhaven National Laboratory, Upton, New York 11973, USA*
[3]*Advanced Photon Source, Argonne National Laboratory, Argonne, Illinois 60439, USA*

(Received 14 August 2009; revised manuscript received 11 September 2009; published 22 October 2009)

Pentaphenyl trimethyl trisiloxane is an isotropic liquid at room temperature with a dynamic glass transition at 224 K. Using x-ray reflectivity, we see surface density oscillations (layers) develop below 285 K, similar to those seen in other metallic and dielectric liquids and in computer simulations. The layering threshold is ~0.23 times the liquid-gas critical temperature. Upon cooling further, there is a sharp increase at 224 K in the persistence of the surface layers into the bulk material, i.e., an apparently discontinuous change in static structure at the glass transition.

DOI: 10.1103/PhysRevLett.103.175701 PACS numbers: 64.70.kj, 68.03.Hj

It is generally accepted that there is no significant difference between the static structures of the glass and liquid states of a given material [1]. Both have isotropic, short-range point-point correlations. The question we address here is whether the conventional wisdom still applies when a region of the liquid is not isotropic. It is now known that bulk-isotropic liquids can have anisotropic order (layers) near their free surfaces at sufficiently low temperatures [2–9]. Does symmetry-breaking in the liquid permit the observation of differences between the static structures of liquids and glasses?

Surface layering has now been seen in liquid metals (e.g., Hg [2], Ga [3], In [4], Sn [5], and Bi [6]), in computer simulations of liquids without an electron gas [7,8], and in one dielectric liquid, tetrakis(2-ethylhexoxy)silane (TEHOS) [9]. While it is possible that metallic liquid layering is driven by different physics (i.e., is an effect of the electron gas [10]), parsimony favors a common explanation. The layering criterion obtained from simulations [7], $T< \approx 0.2T_c$ where T_c is the liquid-gas critical temperature, roughly matches the onset of layering in TEHOS at $T \approx 0.23T_c$, and it is also consistent with all liquid metal data since these have very high T_c but were studied only below the predicted thresholds.

If surface layering at lower temperatures is a general property of ''isotropic'' liquids (although unobservable if freezing occurs first), it is reasonable to ask how the layering evolves when the material is cooled further. Unfortunately, in many liquids studied previously, the surface roughens substantially at the liquid-solid transition, making it impossible to see any layers [11]. (Surface freezing has been observed in paraffins [12] and a liquid metal mixture [13], but this behavior is distinct from surface layering.)

We have now studied the temperature dependence of surface structure in a bulk-isotropic dielectric liquid, 1,1,3,5,5-pentapheny1-1,3,5-trimethyltrisiloxane (PPTMTS). This material is used as a diffusion-pump oil (Dow Corning 705) because of its ultralow vapor pressure, which is also advantageous for us because our thin film samples do not evaporate. The molecule consists of three Si atoms connected to each other through two oxygen atoms, with attached phenyl rings and methyl groups (dimensions ~10.5 Å max to ~7.5 Å min). It does not crystallize easily, but undergoes a well-characterized dynamic glass transition at $T_g = 224$ K [14]. The boiling point is 523 K at 100 Pa [15]. Using the Clausius-Clapeyron equation to estimate the normal boiling point, and then using the normal boiling point to estimate the critical temperature [16], we find that T_c is ~1210 K (this estimation process has an uncertainty of roughly ±5%). Thus, $T_g < 0.2T_c$, which means that surface layering should not be preempted by freezing in this material.

PPTMTS was purchased from GELEST, Inc. with a nominal purity of 95% and used as supplied. In order to easily cool the liquid in a standard closed-cycle refrigerator and orient its surface in a standard diffractometer, ~1.5 μm films were spread on silicon substrates by spin coating. The liquid film thickness is much larger than relevant length scales (surface roughness, molecular dimensions, etc.). To avoid seeing features due to the liquid-substrate interface, we prepared and used HF-etched substrates with rms surface roughness >20 Å so that the internal interface contributes only a diffuse scattering background [9,17]. Before deposition of liquid films, the cleaned Si wafers were etched once again with 2% HF to make the substrates hydrophobic, which allowed us to get uniform wetting with PPTMTS. We saw no measurable changes in film thickness, uniformity, or wetting properties over at least 3 days.

Specular x-ray reflectivity studies were performed with a beam size of ~0.5 mm vertically and ~1 mm horizontally. The momentum resolution was ~0.004 $Å^{-1}$. The samples were mounted on the cold head of a closed-cycle refrigerator, and the system was pumped with a molecular turbo pump. Slightly off-specular ''background'' scans

were performed and subtracted from the specular data, thus removing the scattering from all diffuse sources including the rough liquid-solid interface.

Figure 1 shows the measured specular reflectivity R divided by the ideal surface (Fresnel) reflectivity R_F at three selected temperatures. At 298 K, the featureless scan indicates that the electron density varies monotonically from liquid to vapor, as in many isotropic liquids [18]. A broad hump in the reflectivity appears when the temperature is lowered, signaling a nonmonotonic electron density near the surface. The onset of this surface structure was found to be at 285 K, which corresponds to $\sim 0.23 T_c$. This T/T_c threshold is close to that seen in TEHOS [9] and in simulations [7]. The third reflectivity scan shown is at 220 K, which is below the glass transition. Here, the peak is much stronger, indicating increased deviations from the monotonic density profile.

The inset to Fig. 1 shows only the peak region, at two neighboring temperatures (223 and 225 K). The change in the shape of the reflectivity as a function of temperature is quite abrupt, and it happens across the glass transition ($\sim$224 K). These changes appear at the same temperatures whether we are going up or down, and do not have any detectable dependence on age or temperature history of the sample, x-ray exposure, etc.

Reflectivity data were fitted with the distorted crystal model (DCM), commonly used in liquid metal studies [19,20]. Here, the density $\rho(z)$, averaged over the x and y directions, consists of a semi-infinite series of Gaussians with increasing widths. This model density is used to calculate the reflectivity [21], and the parameters in it are varied to obtain the best fit to the data. As with the liquid metals Sn [5] and Bi [6], we found it necessary to include a density enhancement at the surface. Thus, we assume that

$$\frac{\rho(z)}{\rho_{\text{bulk}}} = r \sum_{n=0}^{n=1} \frac{d_0}{\sqrt{2\pi}\sigma_n} e^{-(z-nd_0)^2/2\sigma_n^2} + \sum_{n=2}^{\infty} \frac{d_1}{\sqrt{2\pi}\sigma_n} e^{-[z-(n-2)d_1-2d_0]^2/2\sigma_n^2} \quad (1)$$

where ${\sigma_n}^2 = \sigma_0^2 + n\bar{\sigma}^2$.

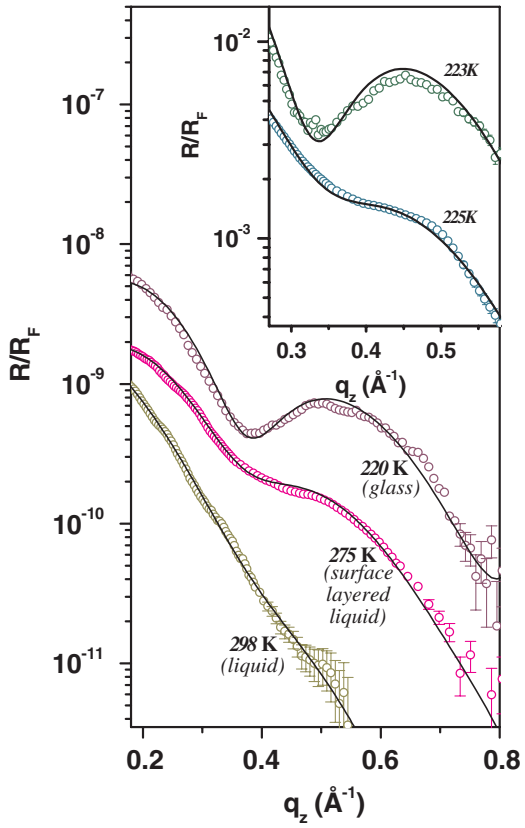

FIG. 1 (color online). Examples of specular reflectivity data (divided by R_F, the theoretical reflectivity from an ideal surface) for $\sim$15 000 Å PPTMTS films. Lines are best fits from which the electron density profiles (Fig. 3) are determined. *Inset:* Peak region of the reflectivity just above and just below the bulk glass transition. (Scans have been shifted vertically for clarity.)

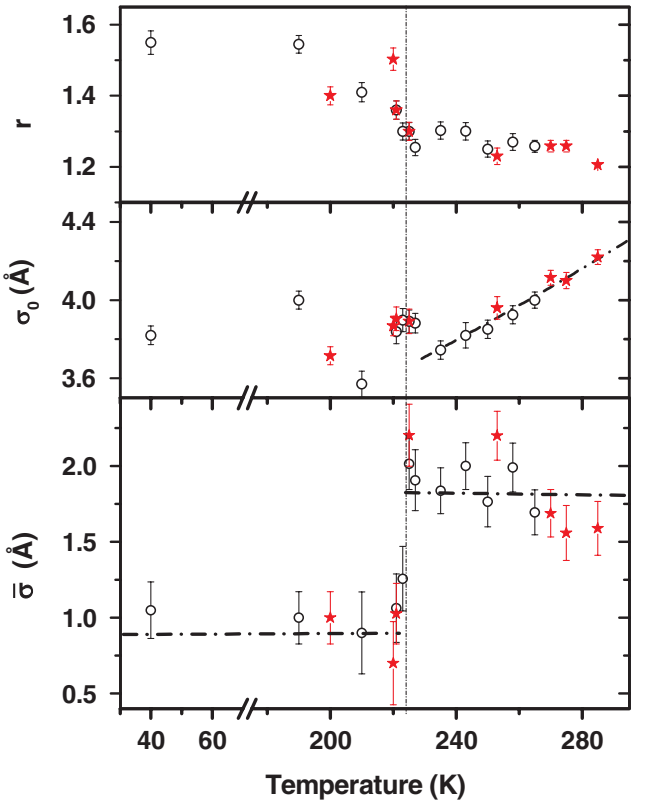

FIG. 2 (color online). Temperature dependence of some fitting parameters (see Eq. 1). *Top:* Surface density enhancement parameter r. *Center:* σ_0 (measures the top surface roughness). *Bottom:* $\bar{\sigma}$ (measures how rapidly the layers broaden as one goes into the bulk). T_g (from Ref. [14]) is shown by the vertical dashed line. Symbols indicate the temperature history of the sample (○: T was lowered to value shown; ★: T was increased to value shown).

The width of the first layer is σ_0, and subsequent layers become increasingly diffuse at a rate determined by $\bar{\sigma}$ (if $\bar{\sigma} = 0$, the layering will be long range). The first layer width σ_0 is composed of a width σ_{cw} due to thermal capillary waves and an intrinsic term σ_i due to nonthermal effects so that $\sigma_0^2 = \sigma_i^2 + \sigma_{\mathrm{cw}}^2$. We have measured the surface tension in the range 265–293 K, extrapolated the data [22], and used this to calculate σ_{cw} [23]. The first two layers may have a different density (multiplicative factor r) and different spacing (d_0) compared to subsequent layers (spacing d_1).

Figure 2 shows the trends in some fitting parameters. Layer spacings are not shown because they do not vary significantly: $d_0 \approx 7.8$ Å and $d_1 \approx 7.5$ Å. The surface density enhancement r (Fig. 2, top panel) shows no specific signal at T_g. The top surface roughness σ_0 (Fig. 2, center panel) increases with T in the layered liquid phase, as expected because of thermal capillary waves. The line through the data shows $\sigma_0(T) = \sqrt{\sigma_i^2 + \sigma_{\mathrm{cw}}^2(T)}$ as defined previously, with a constant best-fit value $\sigma_i = 2.2$ Å and a temperature-dependent capillary width $\sigma_{\mathrm{cw}}(T)$ determined from the surface tension. The result is an excellent fit to the data above T_g. Of course, this equation does not apply once the system dynamics are sufficiently slow. Near and below T_g, there is some variability, but the roughness does not increase significantly near the transition, and this allows us to obtain useful information below T_g.

The most interesting parameter, $\bar{\sigma}$, is shown in the bottom panel of Fig. 2. The horizontal lines are guides to the eye. We see an abrupt (apparently discontinuous) change in $\bar{\sigma}$ by a factor of 2 at the glass transition. This makes quantitative what the peak shapes in Fig. 1 imply, namely, that the layers penetrate further into the bulk when $T < T_g$.

Our samples were held at the desired temperature for at least 30 min before collecting x-ray data. The reflectivity and background scans took another 30–60 minutes at each temperature. At these time scales, our data are the same whether the temperature was raised or lowered to the set point. The time scale of these studies is not easily varied—the measurement cannot be speeded up very much, and orders-of-magnitude longer equilibration times are impractical because of limited beam time. The reversibility of the data suggests that our time scales are long compared to the time scales of this system. However, we saw no Bragg peaks or other evidence of crystallization.

Impurities in liquids are mobile, and therefore of much more concern than in hard-surface studies. Even the highest-purity metallic or dielectric liquids available have far more impurities than necessary to saturate the surface if the impurities were to migrate there. However, that process would decrease the surface energy (surface tension), which would increase the thermal capillary wave amplitude and thus increase the surface width [9]. We saw no such trend within the liquid phase (Fig. 2, center panel). There is also no reason for impurities to appear at the surface suddenly at the bulk glass transition.

Figure 3 shows the densities $\rho(z)$, determined as discussed above, at the same three temperatures as in Fig. 1 (main panel). The solid lines are the actual best-fit electron density profiles; the dashed lines are the same density functions, except with $\sigma_{\mathrm{cw}} = 0$. In other words, the dashed lines show what the surface profiles would look like if thermal capillary waves could somehow be switched off. This visually enhances the density oscillations, but the liquid surface tension cannot really be extrapolated past T_g. Therefore, the insets are used to show that oscillations are present even in the actual density profile.

We conclude that surface oscillations penetrate much more strongly into the bulk of the glass than into the bulk of

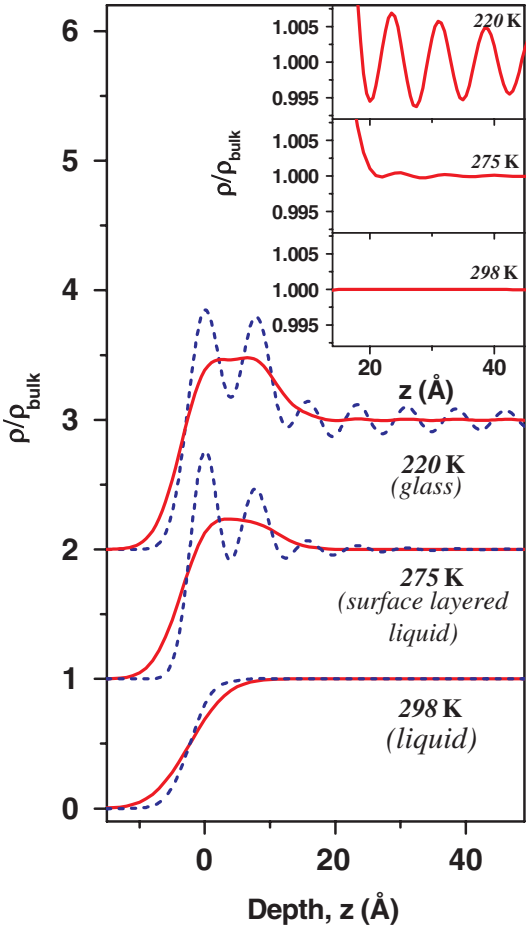

FIG. 3 (color online). Solid lines (red) show best fit normalized electron density functions ($\rho(z)/\rho_{\mathrm{bulk}}$) for ~15000 Å PPTMTS films at the same temperatures as in Fig. 1. The dashed lines (blue) show the density functions with capillary broadening removed (i.e., plotted with $\sigma_{\mathrm{cw}} = 0$). The profiles have been shifted vertically for clarity. *Inset:* density profiles ~20–45 Å below the surface (i.e., in the "deep surface" region), without removal of capillary broadening.

the surface-layered liquid (Fig. 3). To our knowledge, this is the first observation of a sharp change in the static structure at a glass transition. This result does not completely change the conventional view of the bulk structure of glasses; it happens only near a surface. The decrease in $\bar{\sigma}$ is finite, and there is nothing to indicate long-range order (where $\bar{\sigma} = 0$). Nonetheless, it is a significant change that contradicts the widespread notion that nothing happens structurally at T_g.

These results involve an interaction between two apparently distinct phenomena, liquid surface layering and glass formation, neither of which is well understood. Model density oscillations at free liquid surfaces are commonly obtained using density functional theory (DFT) [24–27]. These predictions have fallen out of favor because room-temperature experiments [17] consistently failed to observe oscillatory density profiles in dielectric liquids. Today, we know [7,9] that room temperature is too warm for dielectric liquids; layers are seen when these liquids are cooled to below $\sim 0.2T_c$. Thus, DFT deserves to be revisited.

In general, the predictions of DFT depend on positional correlations, but not necessarily only on the point-point correlations. In glasses, information that distinguishes a liquid from a glass is thought to be contained in ''point-set'' correlations [1], which better characterize the ''amorphous order'' of glasses. This is one example of potentially significant ''hidden'' static and dynamic correlations. We speculate that these correlations, while invisible to direct measurement, reveal themselves by modifying the surface layers, and that DFT may offer a framework through which to understand this coupling.

There are other relevant aspects of the glass transition, and other models of the glassy state. Our comments are not intended to exclude these possibilities. We hope that efforts to understand the phenomenon we report here will provide a test of the various competing theoretical models of glasses.

We acknowledge advice and assistance from Haiding Mo, Claudio Maggi, and Bulbul Chakraborty. This work was supported by the U.S. National Science Foundation under Grant No. DMR-0705137. We used the facilities of the Center for Functional Nanomaterials (CFN), the National Synchrotron Light Source (NSLS), and the Advanced Photon Source (APS), all of which are supported by the U.S. Department of Energy.

[1] A. Cavagna, Phys. Rep. **476**, 51 (2009).
[2] E.g., O. M. Magnussen *et al.*, Phys. Rev. Lett. **74**, 4444 (1995).
[3] M. J. Regan *et al.*, Phys. Rev. Lett. **75**, 2498 (1995).
[4] H. Tostmann *et al.*, Phys. Rev. B **59**, 783 (1999).
[5] O. G. Shpyrko *et al.*, Phys. Rev. B **70**, 224206 (2004).
[6] P. S. Pershan *et al.*, Phys. Rev. B **79**, 115417 (2009).
[7] E.g., E. Chacón, M. Reinaldo-Falagan, E. Velasco, and P. Tarazona, Phys. Rev. Lett. **87**, 166101 (2001).
[8] D. Li and S. A. Rice, J. Phys. Chem. B **108**, 19640 (2004).
[9] H. Mo *et al.*, Phys. Rev. Lett. **96**, 096107 (2006); Phys. Rev. B **76**, 024206 (2007).
[10] S. A. Rice, Proc. Natl. Acad. Sci. U.S.A. **84**, 4709 (1987).
[11] Oleg Shpyrko (personal communication).
[12] E.g., X. Z. Wu, E. B. Sirota, S. K. Sinha, B. M. Ocko, and M. Deutsch, Phys. Rev. Lett. **70**, 958 (1993); X. Z. Wu *et al.*, Science **261**, 1018 (1993).
[13] O. G. Shpyrko *et al.*, Science **313**, 77 (2006).
[14] C. Maggi, B. Jacobsen, T. Christensen, N. B. Olsen, and J. C. Dyre, J. Phys. Chem. B **112**, 16320 (2008).
[15] *A User's Guide to Vacuum Technology*, edited by John F. O'Hanlon (John Wiley & Sons, Inc., New York, 1989), 2nd ed., p. 242.
[16] K. M. Klincewicz and R. C. Reid, AIChE J. **30**, 137 (1984).
[17] C. J. Yu *et al.*, Phys. Rev. E **63**, 021205 (2001).
[18] E.g., B. M. Ocko, X. Z. Wu, E. B. Sirota, S. K. Sinha, and M. Deutsch, Phys. Rev. Lett. **72**, 242 (1994); M. K. Sanyal, S. K. Sinha, K. G. Huang, and B. M. Ocko, Phys. Rev. Lett. **66**, 628 (1991); W. Zhao *et al.*, J. Chem. Phys. **97**, 8536 (1992); W. Zhao *et al.*, Phys. Rev. Lett. **70**, 1453 (1993); A. Braslau *et al.*, Phys. Rev. Lett. **54**, 114 (1985).
[19] O. Shpyrko *et al.*, Phys. Rev. B **67**, 115405 (2003).
[20] E. DiMasi, H. Tostmann, B. M. Ocko, P. S. Pershan, and M. Deutsch, Phys. Rev. B **58**, R13419 (1998).
[21] P. S. Pershan and J. Als-Nielsen, Phys. Rev. Lett. **52**, 759 (1984).
[22] E.g., J. Maroto, F. J. de las Nieves, and M. Quesada-Perez, Eur. J. Phys. **25**, 297 (2004).
[23] E.g., F. P. Buff, R. A. Lovett, and F. H. Stillinger, Phys. Rev. Lett. **15**, 621 (1965).
[24] R. Evans, J. R. Henderson, D. C. Hoyle, A. O. Parry, and Z. A. Sabeur, Mol. Phys. **80**, 755 (1993).
[25] E.g., R. Checa, E. Chacón, and P. Tarazona, Phys. Rev. E **70**, 061601 (2004); J. Winkelman, J. Phys. Condens. Matter **13**, 4739 (2001).
[26] M. E. Fisher and B. Widom, J. Chem. Phys. **50**, 3756 (1969).
[27] P. Tarazona, E. Chacón, and E. Velasco, Mol. Phys. **101**, 1595 (2003).